

Efficient Method for Predicting Rotor/Stator Interaction

S. H. Chen,* A. H. Eastland,† and E. D. Jackson‡
 Rockwell International Corporation, Canoga Park, California 91303

Many modern turbomachinery blade failures are attributed to high vibratory stresses arising from the interactions between stationary and rotating blade rows. A number of finite difference methods have been developed to predict the interaction within a coupled rotor-stator pair. However, these methods cannot currently be used efficiently in a design and development stage. An alternative approach by using a frequency-domain potential paneling method was developed to predict the forced responses due to rotor-stator interaction. In this approach, the rotor and stator are decoupled and their forced responses are solved separately. The forced response on the downstream blade row is simulated by a single blade row with an unsteady nonuniform inflow. Lakshminarayana's wake model was employed as the unsteady forcing function. The unsteady loading on the upstream blade row due to the downstream blade row is assumed to be purely potential. A pseudounsteady approach is used to avoid wake cutting. The nonlinear perturbation is assumed to be much smaller than the mean loading, and only deterministic unsteadiness is considered. The United Technologies Research Center large-scale turbine, which has been used extensively to study rotor/stator aerodynamic and thermodynamic interactions, is revisited here to demonstrate the present capability. The comparison between the predicted results and measurement is very encouraging. The computational time is much smaller than other similar finite difference calculations.

Nomenclature

\bar{B}_{ij}	= surface steady source influence matrix
\tilde{b}_{ij}	= surface unsteady source influence matrix
\bar{C}_{ij}	= surface steady doublet influence matrix
C_p	= pressure coefficient
\tilde{c}_{ij}	= surface unsteady doublet influence matrix
l	= blade index counted outward from reference blade
m	= harmonic index
p	= blade surface static pressure
p_T	= upstream blade inlet total pressure
p_z	= individual blade row inlet static pressure
r	= blade radius
t	= time
U	= freestream velocity
U_m	= far upstream mean x -component velocity
V_m	= far upstream mean y -component velocity
\bar{v}_{nj}	= steady surface normal velocity
\tilde{v}_{nj}	= unsteady surface normal velocity
\bar{W}_{iw}	= wake steady doublet influence matrix
\tilde{w}_{iw}	= wake unsteady doublet influence matrix
Δu_x	= x -component unsteady velocity
Δu_y	= y -component unsteady velocity
$\Delta \theta_x$	= phase angle of Δu_x
$\Delta \theta_y$	= phase angle of Δu_y
$\Delta \varphi$	= inter-wake-element phase angle
δ_{ij}	= Kronecker Delta function
ρ	= density
ϕ	= velocity potential
Ω	= rotational speed
ω_0	= fundamental excitation frequency

Subscript

st	= steady state
T	= overall value
un	= unsteady state

-	= steady value
~	= unsteady value

Introduction

HIGH dynamic forces and the resulting vibratory stresses caused by interactions between rotating and stationary blade rows have been considered a major cause of blade cracks in many modern high-efficiency, high-power turbomachines. For a long-life turbomachine design, the vibratory stresses must be maintained below certain limits to avoid high-cycle fatigue failures. Prediction of vibratory stresses relies heavily on the accurate calculation of unsteady fluid dynamic forcing functions due to the interactions between rotating and stationary blade rows. The rotor-stator interaction calculation represents one of the most challenging problems in fluid mechanics because of the complex geometries involved and the nature of the flow unsteadiness due to relative motion between blade rows. Progress in using high-speed computers enables the physics of the interaction between the rotor and stator to be understood to a great extent by solving the Navier-Stokes equations within a coupled rotor/stator stage.¹⁻⁶ The methods for coupled rotor-stator solutions have been shown to be accurate in predicting both the mean and fluctuating pressures. However, they are still unable to be used efficiently and effectively in the design process due to the constraints of computational efficiency and the use of simplified rotor to stator blade number ratio for calculation. Giles⁷ and Lewis et al.⁸ solved Euler equations with time- or phase-lagged periodic boundary conditions at the periodic boundaries and along part of the overlapped boundaries. Their computational domains consist of only one rotor passage and one stator passage. This greatly removed the limitations found in Refs. 1-6. The computational times are reduced by a factor of more than 10.

A frequency-domain source-doublet-based potential paneling method that predicted the forced response on a blade row due to inflow distortion has been shown in the first author's previous papers.⁹⁻¹¹ This article is an extension of the earlier studies and will show that the forced response in a turbomachinery stage can be calculated accurately by this frequency-domain potential paneling method with a computational speed many times faster than Navier-Stokes, or Euler calculations.

Received July 26, 1992; revision received July 27, 1993; accepted for publication Oct. 21, 1993. Copyright © 1993 by the authors. Published by the American Institute of Aeronautics and Astronautics, Inc., with permission.

*Member of Technical Staff, Rocketdyne Division. Member AIAA.

†Manager, Rocketdyne Division, Fluid Dynamics.

‡Director, Rocketdyne Division, Design Technology.

In the present approach, a rotor/stator stage is decoupled into two separate blade rows. Each blade row interacts only with the immediate downstream or upstream blade row. The influences from other blade rows are assumed to be much smaller than those from the immediate neighboring blade rows, and are neglected.

The downstream blade row forced response is simulated in the traditional manner for blade-wake interaction. It is generally accepted that the wakes shed from the upstream rows have a pronounced unsteady effect on the downstream rows as they convect through the blade passage. This has been noted by many researchers.¹²⁻¹⁸ Hodson¹⁷ and Giles¹⁸ also showed that the blade-wake interaction is essentially inviscid despite the fact that wakes are generated by the upstream blades (rotor or stator) as a consequence of viscous effects. Thus, the incoming wake velocity field can be imposed as the inlet unsteady boundary conditions.

The wake profile can be an analytical or a measured time or spatially dependent velocity distribution. The velocity distributions are generally not simple harmonic. Harmonic amplitudes and related phase angles of this nonsimple harmonic wake field can be obtained through a Fourier decomposition of the velocities. Meaningful unsteady amplitudes and their phases are selected for unsteady loading analysis. An interblade phase angle to account for the phase lag or lead between neighboring blades is imposed to simulate the exact number of blades for rotor and stator. Both measured velocity profiles⁹ and analytical velocity profiles¹⁰ have been used for the flow simulation and are very successful. The same approach is again used in the present study for a rotor/stator interaction analysis.

Reducing the space between turbomachinery blade rows is the trend in designing high-performance turbomachines. As a result, not only the influence from the upstream (specifically the viscous wake effect) is strong, but also the influence from the downstream blade rows may also be significant, especially near the trailing edges. The trailing edges for most blade configurations are thin, but the dynamic pressures excited by the downstream blades are high. This frequently introduces high vibratory stresses and leads to fatigue failures initiated from the trailing edges. Thus, an accurate prediction of the dynamic pressures due to the downstream blade row(s) effect is very important, especially in the design and development stages.

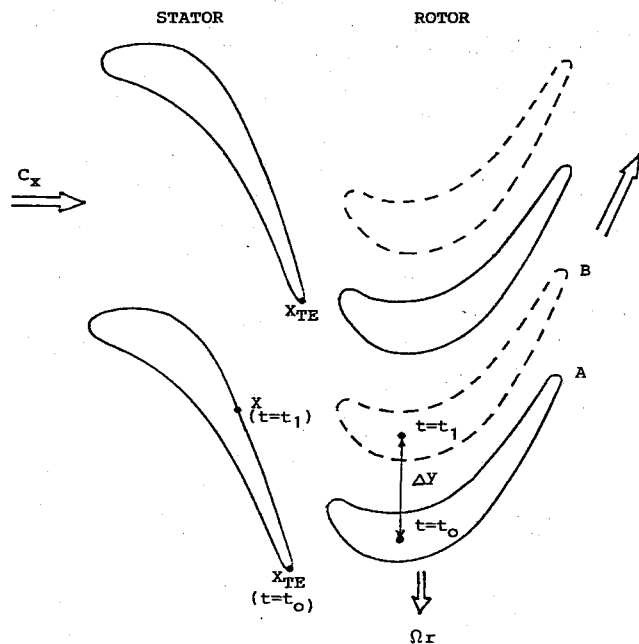


Fig. 1 UTRC large-scale turbine stage.

The relative movement of blade rows causes the downstream blades to cut through the wakes of the upstream blades. The calculation of the forced response of the upstream blades uses a pseudounsteady approach to avoid the wake cutting problem encountered when using a frequency-domain analysis. In this approach, the interaction is assumed to be purely potential. The nonlinear perturbation is assumed to be much smaller than the mean loading. Thus, only a deterministic unsteadiness is calculated. In this calculation, the steady potential of the rear blades is used. However, a backward tracing of the downstream blades is adopted in calculating the influence coefficients to account for a time-dependent effect and minimize the loss of accuracy.

The United Technologies Research Center (UTRC) large-scale turbine test case, Fig. 1, used by Dring et al.¹⁹⁻²¹ to study the flow physics due to rotor-stator interaction has been employed by many other researchers^{1,3-6} to verify their computational algorithms. The same case will also be used here as a basic test case to demonstrate the present capability.

Theoretical Formulation

The present method is a two-dimensional, frequency-domain, inviscid, incompressible potential flow analysis. The detailed formulation has been described by Chen.⁹ Basically, in this method, the steady and unsteady doublet strengths ϕ and $\dot{\phi}$, respectively, are solved separately from the following two sets of simultaneous equations:

$$[\delta_{ij} - \bar{C}_{ij}]\{\phi_j\} - [\bar{W}_{iw}]\{\Delta\phi_w\} = [\bar{B}_{ij}]\{\bar{v}_{nj}\} \quad (1)$$

$$[\delta_{ij} - \bar{c}_{ij}]\{\dot{\phi}_j\} - [\bar{w}_{iw}]\{\Delta\dot{\phi}_w\} = [\bar{b}_{ij}]\{\bar{v}_{nj}\} \quad (2)$$

The influence coefficient matrices include the influences from all the elements on blades and wakes with relative interblade phase angles. The boundary condition on the blade surface is the standard solid wall nonpenetrating condition. The time-dependent freestream velocity

$$U(x, t) = (U_m + \Delta u_x \exp\{i[\Delta\theta_x + m\omega_0\tau \pm (l-1)\sigma]\})i + (V_m + \Delta u_y \exp\{i[\Delta\theta_y + m\omega_0\tau \pm (l-1)\sigma]\})j \quad (3)$$

and the surface unit normal determine the normal velocity ($v_n = -U \cdot n$) on blade surface, where τ equals $t - x_j/U_m$, and σ is the interblade phase angle. The downstream wake doublet strength is expressed in terms of wake doublet strength on the wake panel next to the trailing edge

$$\Delta\dot{\phi}_w(l, k) = [\Delta\dot{\phi}_{wTE}(l)]\exp[-i(NT - k)\Delta\phi] \quad (4)$$

where NT denotes current time step, and k denotes any time step at which the wake elements were generated. Closure is provided by assuming that the wake doublet strength is equal to the velocity potential discontinuity at the trailing edge of the blade.

The downstream blade unsteady load is predicted in a traditional blade-wake interaction manner in which the upstream blade effect is replaced by a convected wake with nonuniform velocity distribution. The wake is a periodic unsteady excitation source to the downstream blade. The wake model generated by Lakshminarayana²² is used in the present case to simulate the wake shed by the upstream blade. The wake profile, Fig. 2, is represented by velocity distribution as a function of axial distance downstream from the trailing edge. The wake used in the present analysis is symmetric with respect to the wake centerline for both axial and tangential velocity components. The profiles have Gaussian distribution near the centerline.

The unsteady calculation is repeated several times for different harmonics. The number of harmonics for unsteady analysis entirely depends on the wake profile, the accuracy requirement, and the turbomachinery operating conditions.

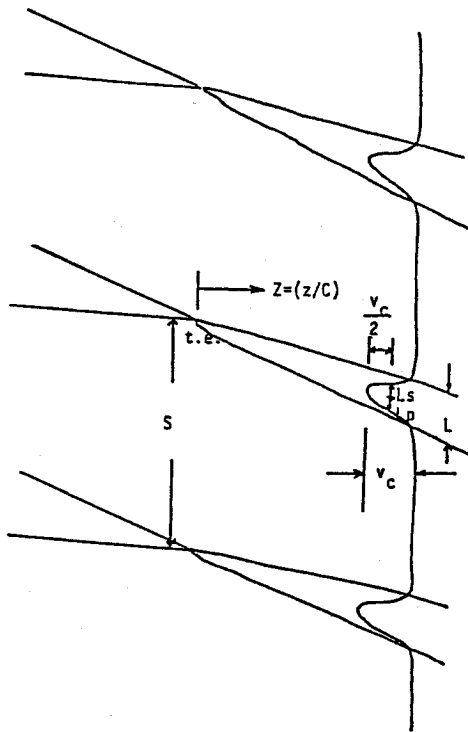


Fig. 2 Lakshminarayana wake profile.

In a time-marching method, the wake generated by the upstream blade row can be traced for each time step as it is convected downstream. After it has been convected a certain length downstream, the wake is chopped by the downstream blades. The wake cutting process can generally be traced accurately as long as the time step is small, however, this requires much more computational time before it comes to a converged periodic solution. In the frequency-domain approach, the path of the wake shed from the upstream blade is prescribed, which unavoidably penetrates the downstream blades. This causes numerical analysis difficulties since the thin wake is mathematically a branch cut and singular doublet sheet. To avoid the numerical problem, a pseudounsteady method is used to calculate the unsteady load on upstream blades.

In this pseudounsteady analysis, we assume 1) The nonlinear perturbation is much smaller than the mean loading, 2) only deterministic unsteadiness is considered, 3) the downstream blade row influence is purely potential and is therefore a strong function of the distance between two blade rows. The effect from the downstream blade row is therefore modeled as a mean potential influence plus a relative distance effect, 4) the downstream blade mean potential is predetermined before the interaction is calculated.

The instantaneous potential influence from the downstream blade row is determined by the relative tangential coordinate between the two blade rows. For this reason, several initial downstream tangential positions over an entire blade pitch relative to the upstream blade row are selected to calculate the strength of these influences. At each initial position, the pseudounsteady influence on a particular point of the upstream blade is calculated by tracing the downstream blades back to its previous position, see Fig. 1. The distance of backward tracing Δy is a function of the mean axial flow convection speed C_x and the rotational speed Ωr

$$\Delta y = \Omega r \cdot t = \Omega r [(x_{TE} - x)/C_x] \quad (5)$$

where x_{TE} is the x coordinate of the upstream blade trailing edge, and x is the x coordinate of the influenced point. This means that if the reference point x_{TE} feels the downstream blades influence from location A at the reference time t_0 , the

point x feels the downstream blade influence as if the downstream blades were at location B a little while ago (t_1). The steady loading on the downstream blade is unchanged, while the influence distance is varied from point to point.

The calculated velocity potential is used to calculate the pressure from the unsteady Bernoulli's equation

$$\frac{p - p_z}{\rho} = -\frac{\partial \phi}{\partial t} - U \cdot \nabla \phi - \frac{1}{2} |\nabla \phi|^2 \quad (6)$$

where ϕ is the superposition of steady potential $\bar{\phi}$ and unsteady potential $\hat{\phi}$ for a particular frequency. The pressure coefficient for that particular frequency is defined as

$$C_{p_{un}}(m) = \frac{p - p_T}{\frac{1}{2} \rho (\Omega r)^2} \quad (7)$$

where m is the harmonic index or the pseudounsteady step. The fluctuation part of the unsteady pressure is obtained by subtracting the steady-state solution, i.e.

$$dC_p(m) = C_{p_{un}}(m) - C_{p_{st}} \quad (8)$$

Overall pressure for the unsteady calculation is the summation of all steady and unsteady pressures

$$C_{p_T} = C_{p_{st}} + \sum_m dC_p(m) e^{i\omega_0 m} \quad (9)$$

The maximum amplitude of pressure fluctuation is defined as the difference between the local maximum and minimum pressures

$$DC_p = C_{p_{max}} - C_{p_{min}} \quad (10)$$

Results

The UTRC large-scale turbine has been used by many CFD researchers^{1,3,6} as a major test case to verify their computational algorithms. This case is also used in the present study to demonstrate the capability of the current methodology. The UTRC large-scale turbine stage has 22 stator blades in the front and 28 rotor blades in the rear. The gap between the two blade rows is 15% of the stator blade chord. The rotational speed is 410 rpm. The axial velocity is 75 fps and the rotational speed is 96.6 fps at midspan.

For a single blade row calculation, only the inflow boundary condition is needed. As the present method is inviscid, the boundary-layer effect is not considered and the outflow pressure may be higher than it should be in real case. The overpredicted outflow pressure can be improved using a simple boundary-layer correction method, or passively match the discharge pressure, if it is available, using the approach described in the next paragraph. It has been shown in Refs. 9–11 that the unsteady loading may not be significantly affected by the accuracy of steady discharge pressure prediction if the boundary layer is not too thick or separated. For a rotor-stator interaction calculation, the flow condition at inflow, outflow, and in between blade rows may be obtained from a reliable gas-path analysis, measurement, or a given design condition. This is to avoid possible inconsistencies when using an inviscid method in which boundary-layer effects and losses are not considered. In the present analysis, the experimental inlet (and discharge) pressures for each blade row are used as input parameters.

With a 15% chord length of stator-rotor separation, the wake velocity defects from the wake model correlation are 20% for the axial component and 25% for the tangential component relative to the stator frame of reference. The amount of tangential velocity deficit is assumed to be preserved from the stator-fixed frame to the rotor-fixed frame. This generates a velocity field as the rotor unsteady inlet boundary condition.

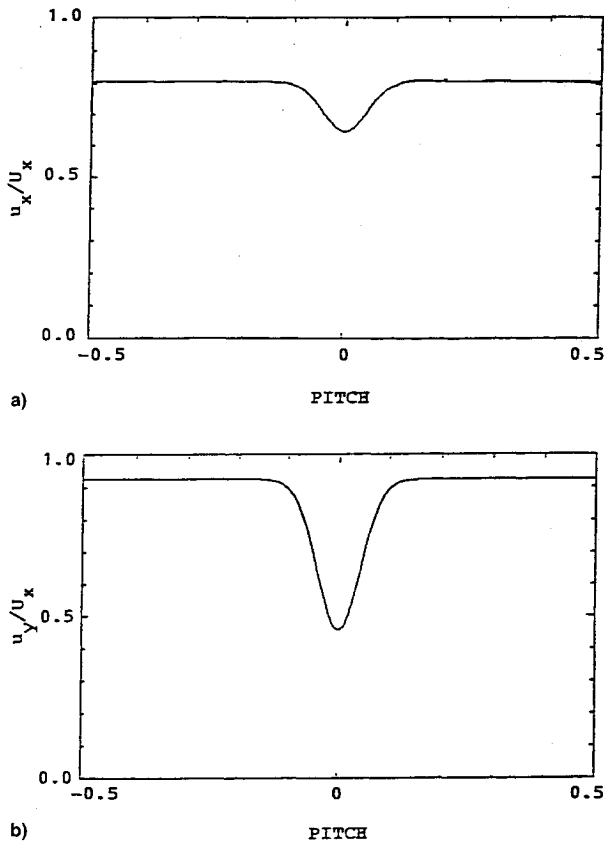


Fig. 3 Stator wake velocity distribution: a) axial component and b) tangential component.

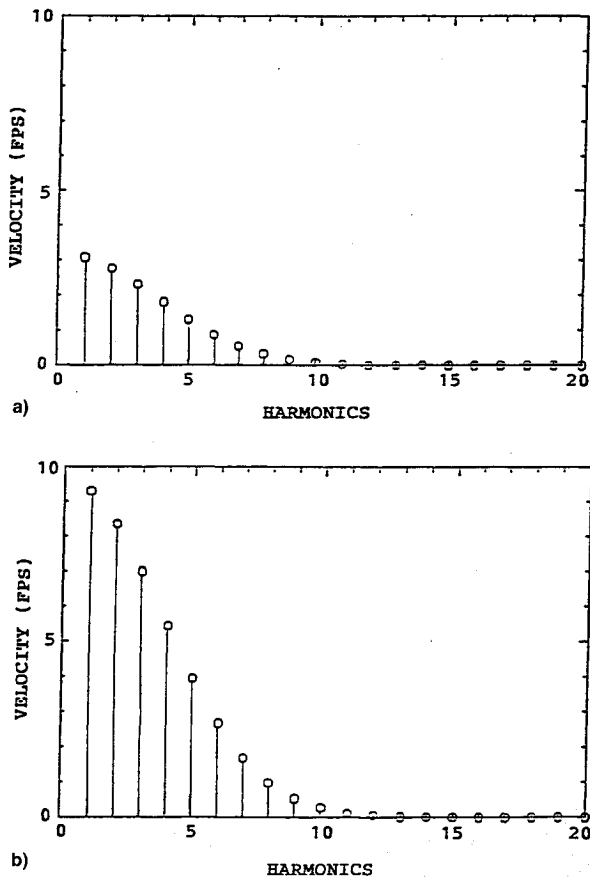


Fig. 4 Harmonic amplitude of stator wake velocity: a) axial component and b) tangential component.

The velocities are shown in Figs. 3a and 3b for axial and tangential components, respectively. The harmonic amplitudes of the wake velocities are shown in Figs. 4a and 4b for the axial and tangential components, respectively. Only the first eight harmonics are picked for analysis. The amplitudes of the higher harmonics are relatively small and are discarded.

Steady-State Pressure Calculation

The calculated steady-state pressures vs nondimensionalized blade chord (0-1 for stator and 1-2 for rotor) are shown in Fig. 5. The pressure distribution compared fairly well with the measured data,¹⁹ except a significant disagreement on the suction side of the stator blade. This is mainly attributed to viscous boundary-layer effects, and in a small way to compressibility effects. There is a significant positive pressure gradient over the aft 40% of the stator blade suction surface. The boundary layer grows much faster in this region than it does on the pressure side. As a result, the predicted discharge pressure is much higher than that measured. The way to remedy the disagreement is to passively change the stator wake influence to match the discharge pressure obtained from measurement.²¹ We can alter the influence by moving the wake cut in either tangential direction in analog to the changing of circulation used in other vortex methods. Better agreement is obtained for the stator as shown by the dotted lines. The stator wake model used in predicting the rotor unsteady response is unaffected.

Unsteady Pressure Calculations

The unsteady pressure fluctuation on the stator is shown in Fig. 6 in which the blade surface is unwrapped with the trailing edge at the center point. The results are based on using four steps to traverse a stator pitch ($N = 4$). The maximum unsteady pressure is near the trailing edge on the suction side which is facing downstream and "sees" the rotor.

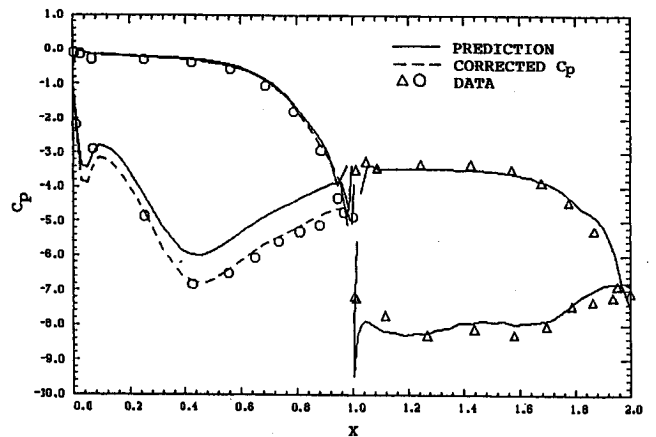


Fig. 5 Steady-state pressure distribution.

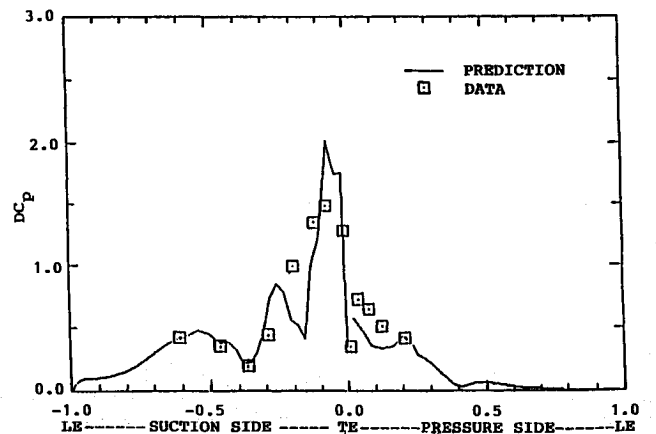


Fig. 6 Stator unsteady pressure fluctuation.

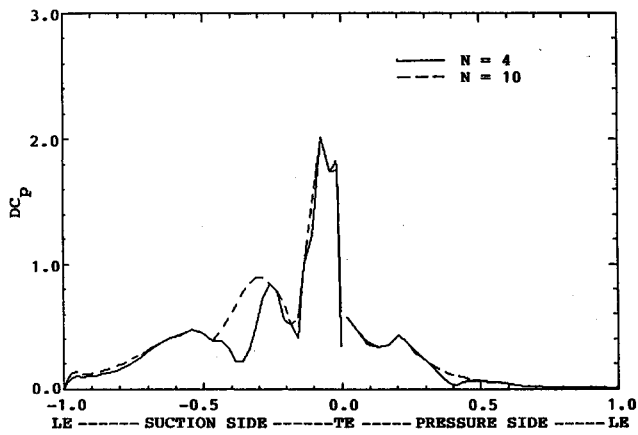
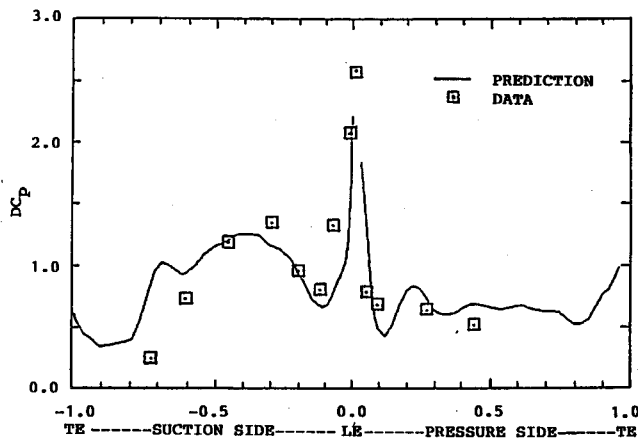
Fig. 7 Effect of N step used in pseudounsteady calculation.

Fig. 8 Rotor unsteady pressure fluctuation.

The amplitude decays rapidly toward the leading edge on both the suction and pressure surfaces. The prediction shows a dip in the dynamic loading at the trailing edge itself, with the minimum loading at 37% axial chord upstream from the trailing edge on the suction surface. These trends agree qualitatively and quantitatively with experimental data.¹⁹ A dip at 18% axial chord upstream from the trailing edge on the suction surface does not show in the data. The decay characteristics of the forced response indicates that the potential effect is the dominant factor in this interaction. The effect of the number of steps used in predicting the stator dynamic loading is shown in Fig. 7. With $N = 4$ and $N = 10$, the two curves essentially have the same prediction except in the region between 55–75% chord on the suction surface. This indicates that a small number of N value will suffice to give accurate dynamic loading predictions using the pseudounsteady calculation.

Eight harmonics of the Fourier decomposed unsteady inlet velocity are used in calculating the rotor forced response. The amplitude of the pressure fluctuations is shown in Fig. 8, where the blade surface is unwrapped with the leading edge at the center. This shows that the maximum amplitude of the unsteady pressure fluctuation is located near the leading edge. The amplitude of fluctuations does not show a monotonic (or near monotonic) decay. This is because the wake effect is a convective rather than a purely potential one. The unsteady pressure is generally larger on the suction surface than on the pressure surface. This is because the low-momentum wake fluid is directed towards the suction surface, the wake velocity deficit therefore creates a larger pressure fluctuation.

Comparisons with three Navier-Stokes calculations^{1,3,6} are shown in Fig. 9 for the stator and in Fig. 10 for the rotor. In Fig. 9 the present method predicted a more rapidly decaying unsteady pressure. This is because we assume the pressure fluctuation is purely due to the rotor potential effect. Qual-

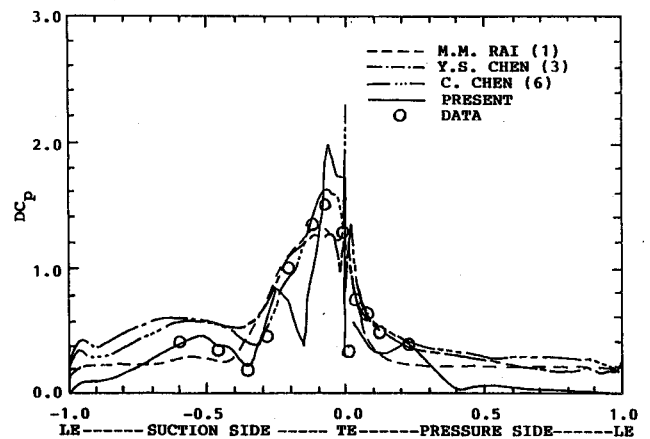


Fig. 9 Comparison of unsteady predictions on stator.

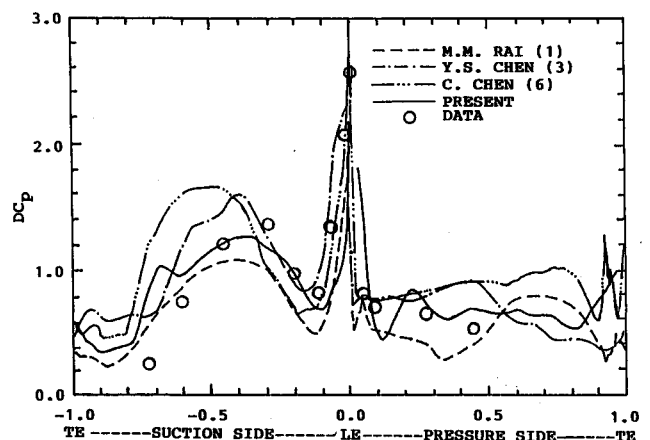


Fig. 10 Comparison of unsteady predictions on rotor.

itatively, all the methods agree quite well with the measurements.¹⁹

Discussions

The results are encouraging in that rotor-stator interaction in a turbomachinery stage can be accurately simulated by decoupling the stage into two separate blade rows with proper wake modeling.

In the present analysis, we adopted a wake model that was developed for isolated blade rows. In the real world, wake fields are changed slightly when a downstream blade row(s) is in place. Before a more sophisticated wake model is developed that takes the nonlinear rotor-stator interactions into account, we assume the convected wake velocity field has already "absorbed" the upstream blade potential influence, whether the gap is big or small.

The wake excitation fundamental reduced frequency for the UTRC rotor is 6.6 based on full chord. The highest reduced frequency for the eighth harmonic used represents 8.4 standing waves on a rotor blade at any instant in time. This indicates an average of less than five grid points within a wave is used for the highest frequency calculation. A qualitative measure of numerical error for high frequencies is the amplitude of the response at high frequency compared to the fundamental frequency (the first harmonic). A large response is often indicative of numerical error rather than pure physical nature. The unsteady amplitude of the 8th harmonic response is observed to be only a small fraction compared to that of the fundamental frequency. This means the numerical error due to each high-frequency excitation is within acceptable limits. It should be noted that the simulation of blade-wake interaction with such a high frequency using a typical finite difference scheme generally requires finer grid, and thus, more computational effort.

The present study is based on incompressible potential flow theory. Despite previous studies that have shown when the boundary layer is not very thick or separated the potential effect dominates, a consistent inflow and outflow boundary condition, especially in between blade-row, for a decoupled rotor-stator interaction calculation should be used. In the present study the experimental inflow and outflow pressures for each blade row are used as input parameters. When in most design applications this experimental data are not available, a reliable gas-path analysis or design condition should be provided for unsteady calculation to avoid possible inconsistent perturbation. An effort to upgrade the present method for compressible flow solutions using density correction scheme is made. This approach with appropriate validation will be shown in future papers.

Computational Time

Using the current methodology, the preprocessing time, the computational time, and the postprocessing time are greatly reduced with little sacrifice of accuracy for both steady and unsteady solutions. The present calculation was performed on an APOLLO DN4000 workstation. Eighty surface panels (forty on the upper surface and forty on the lower surface) and one hundred wake elements for each blade were used. The steady-state pressure calculation consumes less than 10 min in CPU. Two steady-state pressure calculations, four pseudounsteady calculations for stator forced response and eight unsteady rotor forced response calculations took about 2 h DN4000 CPU or just over 1 min equivalent Cray CPU. Compared with a typical Navier-Stokes, finite difference calculation or Euler solution, the savings in cost is obvious.

Summary

A unique approach using a source-doublet-based frequency-domain potential paneling method has been developed to predict turbomachinery rotor-stator interactions. This method decouples a turbomachinery stage and solves the forced responses on rotor and stator separately using appropriate modeling. A pseudounsteady method is used to calculate the upstream blade response due to the potential interaction with the downstream blades. The unsteady response on the downstream blade row is calculated in a typical blade-wake interaction manner. In the case of the UTRC large-scale turbine stage demonstrated, the wake model developed by Lakshminarayana was employed, though a more sophisticated wake model including blade row interactions could be used. Both the forced response on the rotor and the stator compared excellently with experimental data and other finite difference solutions for a coupled rotor/stator stage. Moreover, the computational time is more than 100 times faster in CPU than a typical Navier-Stokes solution. As it is computationally efficient and accurate, it can be used to evaluate multiple design options to optimize a design for dynamic loading.

References

- ¹Rai, M. M., "Navier-Stokes Simulations of Rotor-Stator Interaction Using Patched and Overlaid Grids," AIAA Paper 85-1519, July 1985.
- ²Jorgenson, P. C. E., and Chima, R. V., "An Explicit Runge-Kutta Method for Unsteady Rotor/Stator Interaction," AIAA Paper 88-0049, Jan. 1988.
- ³Chen, Y. S., "3-D Stator-Rotor Interaction of the SSME," AIAA Paper 88-3095, July 1988.
- ⁴Gundy-Burlet, K. L., and Rai, M. M., "Two-Dimensional Computations of Multi-Stage Compressor Flows Using Zonal Approach," AIAA Paper 89-2452, July 1989.
- ⁵Yang, R. J., and Lin, S. J., "Numerical Solutions of Two-Dimensional Multi-Stage Rotor/Stator Unsteady Flow Interactions," Computational Fluid Dynamic Symposium on Aeropropulsion, NASA CP-10045, No. 9-1, April 1990.
- ⁶Chen, C., and Chakravathy, S., "Calculation of Unsteady Rotor/Stator Interaction," AIAA Paper 90-1544, June 1990.
- ⁷Giles, M. B., "Stator/Rotor Interaction in a Transonic Turbine," AIAA Paper 88-3093, July 1988.
- ⁸Lewis, J. P., Delaney, R. A., and Hall, E. J., "Numerical Prediction of Turbine Vane-Blade Aerodynamic Interaction," *Journal of Turbomachinery*, Vol. 111, No. 4, 1989, pp. 387-393.
- ⁹Chen, S. H., "Turbomachinery Unsteady Load Predictions with Nonuniform Inflow," *Journal of Propulsion and Power*, Vol. 8, No. 3, 1992, pp. 667-673.
- ¹⁰Chen, S. H., and Eastland, A. H., "Forced Response on Turbomachinery Blades Due to Passing Wakes," AIAA Paper 90-2353, July 1990.
- ¹¹Chen, S. H., Eastland, A. H., and Boynton, J. L., "Unsteady Pressure Fluctuation on a Highly Loaded Turbine Blade Row," International Symposium on Nonsteady Fluid Dynamics, Toronto, Canada, June 1990.
- ¹²Adamczyk, J., and Carta, F., "Unsteady Fluid Dynamic Response of an Axial-Flow Compressor Stage with Distorted Inflow," Project Squid TR UARL-2-PU, July 1973.
- ¹³Fleeter, S., "Fluctuating Lift and Moment Coefficients for Cascaded Airfoils in a Nonuniform Compressible Flows," *Journal of Aircraft*, Vol. 10, No. 2, Feb. 1973, pp. 93-98.
- ¹⁴Fleeter, S., Jay, R. L., and Bennett, W. A., "Rotor Wake Generated Unsteady Aerodynamic Response of a Compressor Stator," *Journal of Engineering for Power*, Vol. 100, Oct. 1978, pp. 664-675.
- ¹⁵Henderson, R. E., and Shen, I. C., "The Influence of Unsteady Rotor Response on a Distorted Flow Field," *Journal of Engineering for Power*, Vol. 104, July 1982, pp. 683-691.
- ¹⁶Suddhoo, A., and Stow, P., "Simulation of Inviscid Blade-Row Interaction Using a Linearized Potential Code," AIAA Paper 90-1916, July 1990.
- ¹⁷Hodson, H. P., "An Inviscid Blade-to-Blade Prediction of a Wake-Generated Unsteady Flow," *Journal of Engineering for Gas Turbines and Power*, Vol. 107, April 1985, pp. 337-344.
- ¹⁸Giles, M. B., "Calculation of Unsteady Wake/Rotor Interaction," AIAA Paper 87-0006, Jan. 1987.
- ¹⁹Dring, R. P., Joslyn, H. P., Hardin, L. W., and Wagner, J. H., "Turbine Rotor-Stator Interaction," *Journal of Engineering for Power*, Vol. 104, No. 10, 1982, pp. 729-742.
- ²⁰Dring, R. P., Blair, M. F., Joslyn, H. D., Power, G. D., and Verdon, J. M., "The Effects of Inlet Turbulence and Rotor/Stator Interactions on the Aerodynamics and Heat Transfer of a Large-Scale Rotating Turbine Turbulence Model," Pt. I, Final Rept., NASA CR4079, May 1986.
- ²¹Dring, R. P., Joslyn, H. D., and Blair, M. F., "The Effects of Inlet Turbulence and Rotor/Stator Interactions on the Aerodynamics and Heat Transfer of a Large-Scale Rotating Influence Model," Pt. IV, Aerodynamic Data Tabulation, NASA CR 179496, May 1988.
- ²²Lakshminarayana, B., and Davino, R., "Mean Velocity and Decay Characteristics of the Guidevane and Stator Blade Wake of an Axial Flow Compressor," *Journal of Engineering for Power*, Vol. 102, Jan. 1980, pp. 50-60.